

Real-time monitoring of diffusion between laminated polymer films

Vadim V. Krongauz*

DSM Desotech Inc., Fiber Optic Materials, 1122 St Charles Street, Elgin, IL 60120, USA

and William F. Mooney III

E. I. DuPont de Nemours & Co. Inc., Imaging Systems Department, New James Street, Call Box 505, Towanda, PA 18848-0505, USA

and E. Richard Schmelzer†

E. I. DuPont de Nemours & Co. Inc., Computing Division, Experimental Station Laboratory, Wilmington, DE 19880, USA

(Received 14 July 1991; revised 16 March 1993)

Diffusion from one layer of a plasticized polymer film to the adjacent laminated layer is examined. Considering the importance of having a non-destructive, real-time method of monitoring interfacial diffusion, we developed a new spectroscopic technique. In the presented method, one of the two layers of a laminated polymer film is doped with electron-acceptor molecules, 2,4,7-trinitro-9-fluorenone, while the other layer contains a polymer with electron-donating side chains, poly(*N*-vinylcarbazole). As electron-acceptor molecules migrate to the adjacent layer, a charge-transfer complex is formed. The charge-transfer complex has a distinct optical absorption band, which is used in the presented technique to monitor its formation. The kinetics of charge-transfer complex formation is diffusion-controlled, and thus it is used to deduce diffusion coefficients of the mobile electron acceptor in various polymer matrices. The implementation of this technique in monitoring other transport processes is considered as well. Detailed mathematical modelling of the interlayer diffusion process based on the obtained experimental data is presented. Diffusivities found for 2,4,7-trinitro-9-fluorenone tracer in cellulose acetate butyrate, poly(vinyl acetate) and poly(vinyl butyrate) polymer matrices were 5×10^{-9} , 2.5×10^{-9} and $2.5 \times 10^{-9} \text{ cm}^2 \text{ s}^{-1}$, respectively. Diffusivities increase as diffusion from the laminated layer progresses owing to plasticizing of the matrix by the diffusing molecules.

(Keywords: real-time monitoring; interlayer diffusion; numerical modelling)

INTRODUCTION

Composite polymeric films are commonly used in protective coatings, packaging, photography and printing. In all of the applications diffusion of small molecules from one polymer layer to another is an important consideration. A pertinent example is the diffusional loss of plasticizer causing hardening of polymer and thus presenting a problem in the material's long-term use and storage¹⁻³. The interlayer diffusion of plasticizer can also be used to create new materials^{4,5}. We undertook these studies in order to monitor the mobile species in laminated photopolymer films used in industrial holography⁴. In doing so, we developed a new, non-destructive, real-time method for monitoring interlayer diffusion.

There are numerous methods for monitoring molecular transport in polymers. The most traditional ones are based on weight measurements and monitoring the redistribution of isotopic tracers⁶. Techniques based on fluorescence quenching and depolarization are becoming more popular for measurements in solid polymers⁷⁻¹¹.

Pattern photobleaching can be used in determining the transport rate of small molecules in polymer films¹². Light scattering, microscopic and nuclear magnetic resonance methods are useful in some cases⁷. A new method based on the combination of fluorescent (scintillating) and radioactive probes was recently proposed¹³. High-precision techniques for measuring small-molecule diffusion in thin polymeric films that employ a piezoelectric quartz microbalance, a bending beam and laser interferometry have also been reported¹⁴. Straightforward new methods of real-time monitoring of diffusion in thin ($< 50 \mu\text{m}$) polymer films were reported¹⁵⁻¹⁷. However, despite such a variety of available methods, monitoring of molecular transport in polymers remains a difficult, time-consuming task requiring substantial experimental and computational sophistication. Diffusion measurements become particularly complicated in the case of thin ($< 50 \mu\text{m}$) polymer films.

Only one or two techniques from the above list may be used to measure molecular transport in laminated thin films. Even those, like fluorescence quenching, are very limited in the range of rates and applications and require expensive instrumentation. Yet, the use of laminated polymer films is expanding in such areas as protective coatings for automobiles, electronics and communications. Therefore, the need for a reliable characterization of

*To whom correspondence should be addressed. Formerly at E. I. DuPont de Nemours & Co. Inc., Imaging Research and Development, Experimental Station Laboratory, Wilmington, DE 19880-0352, USA
† Retired

multilayered polymer products increases. We believe that our new real-time non-destructive method based on the use of easily available reagents and standard instrumentation will address industrial requirements. Although our method is not absolutely universal, it encompasses a relatively wide variety of applications and systems. Only minimal alteration of the polymer of interest is required for implementation of our method.

Principle of the technique

In interlayer diffusion measurements we monitor diffusion by following the build-up in concentration of a coloured charge-transfer complex formed by diffusing molecules and immobile pendent groups attached to polymer chains. The polymer containing immobile, pendent electron-donating groups is located in one layer, while the mobile electron acceptor is placed in another layer of the film. The measurements begin immediately after lamination of these two layers. As mobile electron acceptors migrate into the adjacent layer forming charge-transfer complexes (CTC), the optical density of the film at the wavelength corresponding to the CTC absorption increases. The charge-transfer complexes are formed at diffusion-controlled rates¹⁸. The diffusion of polymer chain segments across the interface is relatively slow, with diffusivities ranging from 10^{-11} to 10^{-13} cm² s⁻¹ (ref. 19). Diffusivities characterizing the migration rate of small molecules like trinitrofluorenone in a plasticized polymer matrix vary from 10^{-7} to 10^{-10} cm² s⁻¹ (refs. 5, 14, 16). Since the rate of polymer diffusion into an adjacent laminated layer is so much slower than that of the monomeric molecules, the CTC absorption band formation kinetics is almost entirely determined by the rate of small-molecule diffusion. In the present work the rate of diffusion of mobile electron acceptors in the film initially containing these molecules was, by design, much higher than the diffusion rate in the film containing polymer chains with pendent electron donors.

Mathematical modelling of the small-molecule diffusion between the laminated polymer films could be used with the experimentally determined kinetics of CTC formation to deduce the diffusivities of small molecules in the polymer layers.

EXPERIMENTAL

Materials and reagents

Since in our previous work holographic materials were investigated^{16,17}, we also used photoexposed holographic photopolymer films in this work. Thus, the current results can be compared to our previous data obtained by other techniques^{16,17}. Photopolymer films consist of a support (here Mylar[®]) coated with a plasticized polymer matrix (binder) that contains a photopolymerizable composition dissolved in the plasticizer. Diffusion was monitored in three inert, plasticized polymer matrices: cellulose acetate butyrate (CAB), poly(vinyl acetate) (PVA) and poly(vinyl butyrate) (PVB) (all from Monomer-Polymer and Dajac Laboratories Inc.). Holographic photopolymers contain *N*-vinylcarbazole (NVC) as the major photopolymerizable component. Thus, the resulting poly(vinylcarbazole) (PVCA) or commercially available PVCA (Pfaltz & Bauer Inc.) were used as a polymer containing pendent electron donors. Holographic films used in the measurements were formulated with the binders listed above. 2,4,7-Trinitro-9-fluorenone (TNF)

(Fluka, 98% pure) was used as a mobile electron acceptor. All reagents were used as purchased without further purification. In some experiments the layer containing the immobile donor was prepared using a solution of holographic photopolymer^{4,20} in methylene chloride (EM Science, spectroscopically pure), which was coated on 50 μ m Mylar support film using a doctor-knife, dried for 2 h and then exposed to a full spectrum of 2000 W Xe-arc lamp light and 24 h of heating at 70°C to ensure complete polymerization of *N*-vinylcarbazole. The resulting film was 20 μ m thick. The concentration of PVCA in the resulting film was 8% by weight relative to the total weight of this composite. In other experiments, PVCA and binder, CAB, PVA or PVB (8% of PVCA by weight relative to the binder), were dissolved in methylene chloride and coated to form a 20 μ m film on Mylar support.

To produce the layer with mobile TNF acceptors, ethoxylated phenol monoacrylate (Photomer[®] 4039, Henkel Corp.) and polymer binder (CAB, PVA or PVB) were dissolved in methylene chloride and knife-coated on 50 μ m Mylar film to form a 25 μ m thick coating after drying. The concentration of Photomer 4039 was equal to 40% by weight. Photomer 4039 was selected as plasticizer since it has a low viscosity (15–25 cP, Henkel Corp.) and is extensively used as a reactive postcuring diluent in many holographic photopolymers and photocurable coatings.

Equipment and run procedure

The absorption spectra and time dependence of the absorbance were measured using an IBM u.v./vis. 9420/9430 spectrophotometer. The minimum time interval used in the measurements was 2 s. All experiments were conducted at room temperature, 298 ± 1 K, which remained constant during the experiment. The local temperature increase within the film due to CTC formation was neglected because of the low concentration of the reactants.

The charge-transfer complex formed by TNF and poly(vinylcarbazole) absorbs in the studied polymer matrices, PVA, CAB and PVB, in the region between 480 and 520 nm (*Figure 1*). To observe the migration of Photomer 4039 (plasticizer) and TNF from one film into another, one piece of Mylar film was coated with the polymer matrix containing TNF and Photomer 4039 plasticizer, another piece of Mylar film was coated with fully polymerized holographic photopolymer containing immobile donors (PVCA) or with the film made from pure binder (CAB, PVA or PVB) containing an equivalent amount of PVCA. The films were placed with the coated sides facing each other. A hand roller was used once to gently laminate these films. The samples of laminated film examined under a microscope did not show any air bubbles or other visible signs of imperfect contact between the layers. The laminated film formed as described above was placed into a spectrophotometer immediately after lamination. The change in optical density due to CTC formation caused by diffusion of TNF (along with Photomer) from one layer into another was recorded at the wavelength of 480 nm. Lamination and insertion of the laminated film into the spectrophotometer took on average 9 s. The data were collected for 7 min with the frequency of one measurement every 2 s, and then the frequency was reduced to one measurement every 10 s. The final data points were collected after several

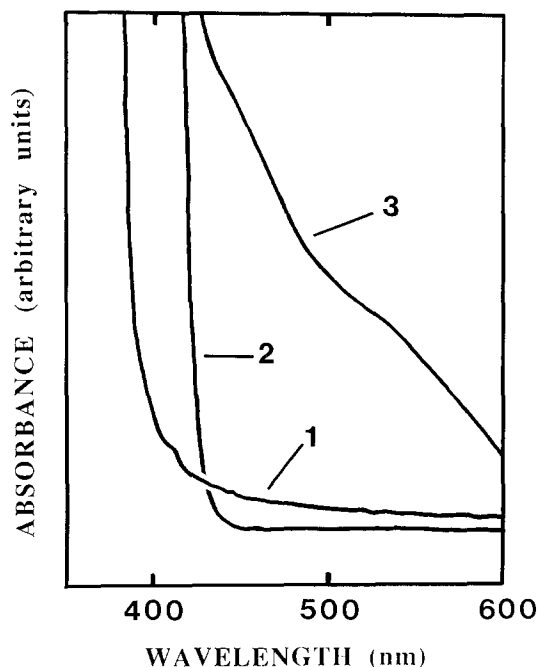


Figure 1 Absorption spectra of (1) the 25 μm film containing mobile electron acceptors, (2) the 20 μm film containing immobile electron donors, and (3) the composition film made by laminating these two films. The absorbance of the laminated films was measured after the diffusion took place and the charge-transfer complex was formed

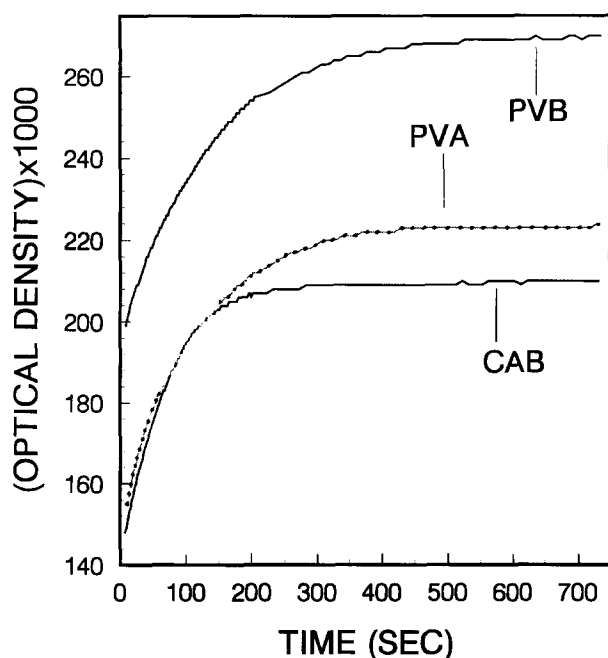


Figure 2 The accumulation of the charge-transfer complex due to diffusion of electron acceptor from the highly plasticized layer to the films made with different polymer matrices

hours to ensure that equilibrium had been reached (*Figure 2*). Data were averaged over three experimental runs for each photopolymer matrix tested.

RESULTS AND DISCUSSION

Charge-transfer complex accumulation kinetics

Diffusion-controlled rates of charge-transfer complex formation were measured in three different polymer

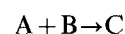
matrices. When a polymer matrix was changed, it was changed simultaneously for both layers: layer A containing the mobile electron acceptor, TNF, and layer B containing the immobile donor, PVCA. The matrices, CAB, PVB and PVA, were selected because small molecules migrate with different rates in these matrices as was previously measured by us using fluorescence methods²¹. The differences were again observed by the presented new method (*Figure 2*). The size of Photomer 4039 molecules is similar to that of TNF, and thus we would expect the migration rates of plasticizer and TNF to be similar. TNF was added as a tracer to obtain information about the diffusion rate of the plasticizer or any other molecule of similar size and polarity. The data on TNF diffusion in various matrices are treated below as the data on mobility of any other tracer designed to imitate the mobile species of interest.

The deduction of diffusivities from the tracer mobility data always requires careful modelling. Indeed, the kinetics depends on the relative values of concentrations of reactive species in films A and B, the difference in TNF diffusion rate in the adjacent films, the interface structure, etc. In addition, with very thin films and high concentrations of donor and acceptor, the fraction of colour formed in the insertion step of the experiment becomes significant. This last difficulty is handled by us in a traditional manner⁶ by normalizing the data to the difference between the final, $OD(\infty)$, and the initial, $OD(0)$, optical densities: $[OD(t) - OD(0)]/[OD(\infty) - OD(0)]$.

Model of the process; initial and boundary conditions

To predict the behaviour of other systems, to understand the process of transport and to compare it with the results of other studies, one has to have a physical and mathematical model of the process. The same model is also essential for the deduction of diffusion coefficients.

In our model, we consider that the pair of films containing the reactive species are in perfect laminated contact. We identify the reactants as A and B (here electron acceptor and electron donor, respectively). These species react irreversibly to produce C, a 'coloured' product (here a charge-transfer complex), which can be quantitatively measured:



Initially A is in one film layer with thickness Δ , while B is in another with thickness Ω . Only one of the reactants is mobile; in the present experiments it is A. It gradually diffuses into the other layer, where it reacts rapidly with B. Amounts of A and B may not be in stoichiometric ratio in the two films. With insufficient A the 'colour' front will never reach the outer film surface (behind the interface). With excess A both films eventually will contain a uniform concentration of A. Diffusive transfer of A in its source film (the interface is selected as a coordinate origin so that $-\Delta \leq x \leq \Omega$) is given by the equation (where we use italic A and B to represent concentrations of reactants A and B):

$$\partial A / \partial t = -D_1 \partial^2 A / \partial x^2 \quad \text{for } -\Delta \leq x \leq 0$$

and in the reactive film

$$\partial A / \partial t = D_2 \partial^2 A / \partial x^2 - kAB \quad \text{for } 0 \leq x \leq \Omega$$

This includes the term for the irreversible reaction that consumes A. The partial differential equation for the

immobile B is restricted to the reactive film:

$$\partial B/\partial t = -kAB \quad \text{for } 0 \leq x \leq \Omega$$

Initial conditions are dictated by the conditions of the experiment (the composition is given above):

$$\text{for } -\Delta \leq x \leq 0 \quad A = A_0 \text{ and } B = 0$$

and

$$\text{for } 0 \leq x \leq \Omega \quad A = 0 \text{ and } B = B_0$$

Boundary conditions for A for the second-order partial differential equation in the spatial variable x are:

$$[\partial A/\partial x]_{-\Delta} = [\partial A/\partial x]_{\Omega} = 0$$

There are no boundary conditions for the variable B since it is not a direct function of x and only changes with x in response to its consumption by A.

There is also an interfacial condition that must be honoured. Contact between the films is assumed perfect and consequently concentrations within the infinitesimally small region, $x = \pm \varepsilon$, near the interface are the same as ε vanishes. Also:

$$[D_1 \partial A/\partial x]_{-\varepsilon} = [D_2 \partial A/\partial x]_{+\varepsilon}$$

These assumptions specify that at physical equilibrium concentrations of A are the same in the two films, but rates of diffusion may be different depending on values of the diffusivities. Of course, diffusivities may be equal. Clearly there is no problem if diffusivities vanish, since the reactants are permanently separated.

The reaction rate constant k , according to the mathematical model, can be 'large' or 'small', changing the relative diffusion and reaction rates. Including the reaction-rate term in the model, rather than making the rate of the complex formation *a priori* infinitely faster than the rate of diffusion, allowed us greater flexibility in the handling of the problem and analysis of the data.

To correlate the computational results with the experimental data, we solved the above equations in the reduced coordinates for the observable variable C, representing the concentration of the charge-transfer complex. Instead of the absolute concentrations, we used those normalized to the difference between the initial and equilibrium concentration of immobile component B since the decrease in B concentration is equal to concentration of the forming coloured product C:

$$C(t)/C(\infty) = [B(0) - B(t)]/[B(0) - B(\infty)]$$

Calculation parameters

Rather than looking for the analytical solution of the system of differential equations presented above, we obtained a numerical solution using realistic values for the parameters defining the interlayer transport described above. Values for all the selected parameters are based on existing experimental data obtained in this laboratory and found in the literature. The set includes the thickness of the films $\Delta = 25 \mu\text{m}$ and $\Omega = 20 \mu\text{m}$.

The diffusion coefficient of the TNF in layer A is larger than that in the second layer containing the immobile PVCA. The method is designed to find the diffusion coefficient in the second film knowing the diffusion coefficient in layer A. The film A initially containing all of the mobile acceptor was highly plasticized. We concluded that the diffusion coefficient for TNF in this film should be close to that of similar size molecules in liquids such as Photomer 4039 and

selected for the model $D_1 = 10^{-7} \text{ cm}^2 \text{ s}^{-1}$. Determination of the diffusion coefficient for the migration within the second film depends on the value of the rate of the colour charge-transfer complex formation, and in the model on the relation of k , concentrations A and B of the reagents and D_2 . It is intuitively obvious that, starting at a certain reaction rate, the process becomes diffusion-controlled. To simplify the analysis of this limit, we solved the normalized equation of the A component's distributions:

$$\frac{\partial(A/A_0)}{\partial(D_2 t/\Omega^2)} = \frac{\partial^2(A/A_0)}{\partial(x/\Omega)^2} - \frac{\Omega^2 k B_0}{D_2} \frac{A}{A_0} \frac{B}{B_0}$$

Since the formation of coloured CTC (C) is determined by the amount of reacted PVCA (B), we solved the above equation for B/B_0 using $\gamma = k B_0 \Omega^2 / D_2$ as a parameter. The diffusional limit is reached at the kinetic parameter $\gamma \geq 100$. The concentration B_0 in our experiments was 8% by weight. Results of earlier reported investigations¹⁵⁻¹⁷ indicate that D_2 varies from system to system from 10^{-3} to $10^{-9} \text{ cm}^2 \text{ s}^{-1}$. Therefore the CTC formation reactions with rate constants in excess of $10^5 \text{ cm}^3 \text{ mol}^{-1} \text{ s}^{-1}$ satisfy the conditions of applicability of the method to our films. The rate constant for the PVCA reaction with TNF is definitely higher than that value¹⁸.

Mobile species distribution in time

We used our model to answer qualitatively the crucial question of mobile-molecule distribution during the concentration equilibrium between two adjacent laminated polymer films. One of the difficulties in monitoring molecular transport in various systems is the lack of high-resolution methods of detecting the spatial distribution of tracer within the media. Modelling is the only way to obtain this information since even the most sophisticated techniques (with rare exceptions^{15,22}) provide information only on bulk changes. We examined the spread of the mobile reactive molecule A through both films under different conditions. Only the case of the diffusion-controlled reaction of charge-transfer complex formation between A and B is considered here.

The example of computed distribution of molecules A is presented in Figure 3. We can observe a gradual decrease of concentration within the film (for distances < 0) initially containing the tracer. Then, a sharp break in the concentration occurs at the interface of the two laminated films. At earlier times, all the A molecules are consumed by reaction with B close to the interface. As the concentration of the immobile B diminishes near the interface, the concentration of A in those regions is increasing. This increase is vividly visible along the lines representing the cross-sections of the A concentration surfaces by the planes parallel to the concentration-time plane. At the end of the process, the uniform concentration of mobile species is established across the interface in the case $A \geq B$ or the entire A species disappears in the case of $B \geq A$. The plots in Figure 3 demonstrate that even in the case of relatively rapid diffusion ($D_2 = 10^{-9} \text{ cm}^2 \text{ s}^{-1}$) and consumption of the mobile species, the equilibration of the mobile species concentration takes some time. The results of our model computations (Figure 3) illustrate why it is necessary to age freshly coated multilayer films (manufactured for imaging, packaging or any other purposes) before their intended use. Indeed, the residual low-molecular-weight formulation components remaining in various layers of these materials will eventually migrate from layer to laminated layer and cause mechanical,

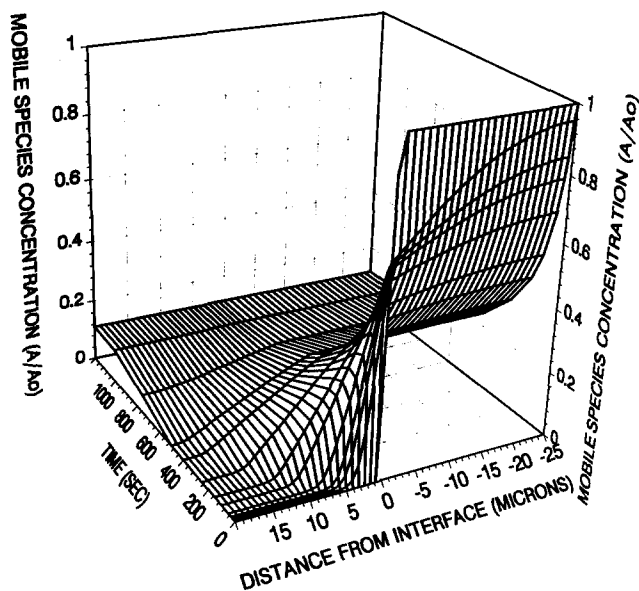


Figure 3 Example of computed change in concentration of mobile reagent (electron acceptor) resulting from interlayer diffusion. Concentrations of mobile and immobile species are equal; however, the total amount of the mobile species is slightly higher than that of immobile species owing to the film thickness difference. Zero on the abscissa axis corresponds to the plane of contact of layers

photochemical and barrier properties to drift away from those measured immediately after production.

The presented mathematical model does not contain the requirement to maintain the concentration of the mobile tracer uniform. The computation of the change in the distribution of the mobile tracer concentration in both laminated layers was one of the prime objections of the presented modelling.

Diffusion coefficient deduction

Experimentally we measured only the total amount of the formed product, C , by its optical density. Using our model we computed product, C , accumulation kinetics as well. The diffusion coefficient D_2 of the mobile species A in our model is considered the only unknown parameter. By varying this parameter in the model computations we found the optimal fit with the experimental data. The goal of the current work was to develop the methodology and to demonstrate the applicability of the approach to the monitoring of interlayer diffusion. Therefore we did not seek the exact values for all the parameters. It was sufficient to operate in the region where the influence of the change in D_1 and k on the computed D_2 is negligible. Using precise values of the complex formation rate constant and the diffusion coefficient of A in the non-reactive layer will allow extension of the range of measurements and the applicability of the method.

The experimental data on optical density increase due to CTC accumulation were normalized to unity and superimposed on the curves computed by varying the diffusion coefficient D_2 , in the film of interest (Figure 4). The value $D_1 = 1 \times 10^{-7} \text{ cm}^2 \text{ s}^{-1}$ was used for the computations presented in Figure 4. This is a reasonable average value for small-molecule diffusivity in a heavily plasticized polymer⁷⁻¹¹. This value of diffusion coefficient also gives the best fit to our experimental data for a wider time range. The plasticized second film was selected to imitate the holographic image modulation process⁴ and

the process of plastics ageing due to plasticizer migration and loss. Drastically different diffusivities of the tracer in plasticized and non-plasticized films also simplified the deduction of tracer diffusivities in matrices containing no plasticizer.

The data obtained for holographic formulations did not differ significantly from those found for the corresponding pure binders containing PVCA. Comparison of the experimental data with the data computed using the diffusion coefficients as parameters (Figure 4) resulted in a quantitative comparison of the rates of TNF migration in various polymer matrices. Thus, the rate of TNF migration in CAB matrix is the highest, while that in PVB is similar to the migration rate in PVA. The diffusion coefficients determined with the current migration model were varying with time. Thus, $D_2(\text{CAB})$ changes from 5×10^{-9} at times less than 50 s to $1 \times 10^{-8} \text{ cm}^2 \text{ s}^{-1}$ at longer times. The diffusion coefficients for PVB and PVA change from about 2.5×10^{-9} at times shorter than 50 s to $5 \times 10^{-9} \text{ cm}^2 \text{ s}^{-1}$ at longer times. This increase in diffusivities is most likely caused by the change in the polymer matrix resulting from the plasticizer and tracer diffusion into it. Swelling and a variable diffusion coefficient⁶ were not included into our model. Our modelling did not require the use of the system with steady-state distribution of the reagent, zero boundary concentration or any other common restrictions^{13,16}, making the results of the diffusion coefficient deduction more realistic. Regardless of the limitations of the mathematical model, the result $D_2(\text{CAB}) > D_2(\text{PVA}) \geq D_2(\text{PVB})$ confirms our earlier measurements of *N*-vinylcarbazole diffusion rate in these matrices, obtained by the fluorescence method²¹. The order of magnitude of these diffusivities, $D_2(\text{CAB}) \approx 7 \times 10^{-9} \text{ cm}^2 \text{ s}^{-1}$ and $D_2(\text{PVA}) \geq D_2(\text{PVB}) \approx 4 \times 10^{-9} \text{ cm}^2 \text{ s}^{-1}$, is also close to those reported earlier for the rate of *N*-vinylcarbazole (similar in size to TNF) migration in these matrices. The values of NVC diffusion coefficients

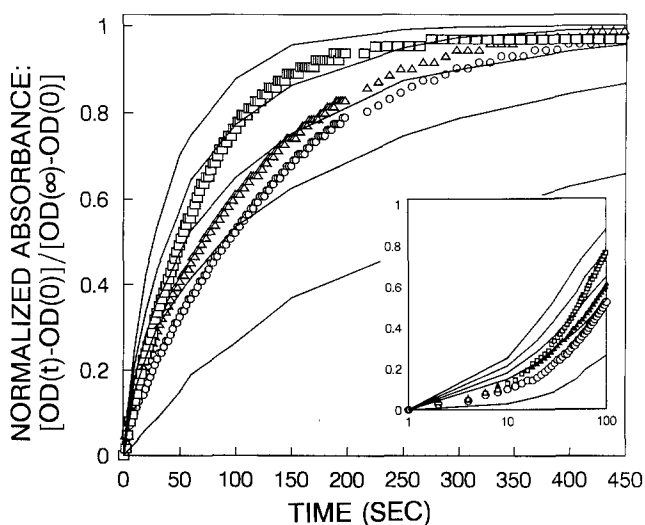


Figure 4 Comparison of the experimentally detected change in the optical density of laminated films with the model computations. The optical density, $OD(t)$, is normalized to the difference between the initial, $OD(0)$, and final, $OD(\infty)$, values: $[OD(t) - OD(0)] / [OD(\infty) - OD(0)]$. The data correspond to the measurements conducted with the following polymer matrices: (\square) CAB, (\triangle) PVA, (\circ) PVB. The full curves correspond to the computations with $A = 1\%$, $B = 8\%$, $D_1 = 1 \times 10^{-7} \text{ cm}^2 \text{ s}^{-1}$, while D_2 was varied as 2.5×10^{-8} (top curve), 1×10^{-8} , 5×10^{-9} , 2.5×10^{-9} , and $1 \times 10^{-9} \text{ cm}^2 \text{ s}^{-1}$ (bottom curve). Short-time data are additionally presented in the inset

determined in the identical holographic polymer formulations by a different technique²¹ were $D(\text{CAB}) = 1.5 \times 10^{-9} \text{ cm}^2 \text{ s}^{-1}$ and $D(\text{PVA}) \approx D(\text{PVB}) = 8.5 \times 10^{-10} \text{ cm}^2 \text{ s}^{-1}$.

The diffusion coefficients determined by the interlayer diffusion monitoring and by the internal fluorescence-based method differ by a factor 4.7, which could be caused by a difference in the size of the probe molecule, concentration of plasticizer in unexposed holographic films or by modelling. However, the difference between the probe diffusivities measured in different matrices is the same in the present investigation using TNF and in previous work based on *N*-vinylcarbazole tracer. This result indicates the validity of the charge-transfer complex formation-based technique for monitoring interlayer molecular mobility in laminated polymeric composites.

CONCLUSION

We presented a new, straightforward technique for real-time monitoring of small-molecule diffusion between adjacent layers of laminated films. The method is based on the formation of a coloured complex between mobile electron-acceptor molecules migrating from one polymer layer to an adjacent one containing immobile electron donor. Our method requires only standard instrumentation, and very little modification of the polymer, and permits a clear interpretation and processing of the data as is presented above. To the best of our knowledge, this is the first time that a direct, non-destructive method of *real-time* monitoring of interlayer diffusion has been described. The method is very sensitive and can be used to monitor interlayer diffusion in extremely thin laminated polymeric films as demonstrated. Unlike the phosphorescence or fluorescence quenching techniques, which are limited by the tracer excited-state lifetimes, our technique can be used in monitoring the transport of molecules over a wide time range. As any other transport monitoring technique, this method requires computer modelling in order to extract the tracer diffusion coefficients. Although the method does not yield experimental data on the spatial distribution of the diffusing molecules, it provides information on the kinetics of establishment of molecular equilibrium between the polymer layers. These kinetic data can be used with the mathematical modelling to deduce the dynamics of spatial redistribution of diffusing species between the laminated layers of the film (Figure 3). The method is applicable to a wide variety of systems. Indeed, many polymeric composites contain groups able to act as electron donor or acceptor and form charge-transfer complexes with appropriate mobile tracers. It is also rather simple to add such an immobile polymer label to composite formulation without significantly altering the properties of the material. The method is not sensitive to the presence of

impurities. The test of our method on films with known properties yields diffusion coefficients similar to those measured by other techniques²¹.

We believe that the presented straightforward and convenient technique for estimating the rate of transport of small molecules between laminated films could become an on-line quality-control tool for many industrial processes. The change of colour due to charge-transfer complex formation caused by molecule migration from layer to adjacent layer can also be used as an ageing indicator for multilayered polymeric composites.

ACKNOWLEDGEMENTS

The work was conducted at the E. I. du Pont de Nemours & Co., Experimental Station Laboratory, Imaging Research and Development Department, in Wilmington, Delaware, USA. The financial support of the project by the DuPont Imaging Research and Development at Towanda, Pennsylvania, is gratefully acknowledged.

REFERENCES

- 1 Elias, H. G. 'Macromolecules', 2nd Edn, Plenum, New York, 1984
- 2 Billmeyer, F. W., Jr 'Textbook of Polymer Science', 3rd Edn, Wiley, New York, 1984
- 3 Perepechko, I. I. and Startseva, L. T. *Dokl. Akad. Nauk SSSR* 1982, **263**(3), 641
- 4 Smothers, U. K., Doraiswamy, K. C., Armstrong, M. L. and Trout, T. J. US Patent 4959283, 1990
- 5 Gulnazarov, E. S., Smirnova, T. N., Tihonov, E. A. and Shpak, M. T. *Ukr. Fiz. Zh.* 1988, **33**(1), 8
- 6 Crank, J. and Park, G. S. 'Diffusion in Polymers', Academic Press, London, 1968
- 7 Guillet, J. E. in 'Photophysical and Photochemical Tools in Polymer Science' (Ed. M. A. Winnik), Reidel, Dordrecht, 1986
- 8 Chu, D. Y., Thomas, J. K. and Kuczynski, J. *Macromolecules* 1988, **21**, 2094
- 9 Belford, G. G., Belford, R. L. and Weber, G. *Proc. Natl Acad. Sci. USA* 1972, **69**(6), 1392
- 10 Shiah, T. Y. and Morawetz, H. *Macromolecules* 1984, **17**, 792
- 11 Shea, K. J., Stoddard, G. J. and Sasaki, D. Y. *Polym. Prepr.* 1984, **27**(2), 344
- 12 Smith, B. A. *Macromolecules* 1982, **15**, 469
- 13 Krongauz, V. V. and Reddy, D. *Polym. Commun.* 1991, **32**, 7
- 14 Tong, H. M. and Saenger, K. L. *J. Plast. Film Sheeting* 1988, **4**, 308
- 15 Kwei, T. K. and Zupko, H. M. *J. Polym. Sci. (A-2)* 1969, **7**, 867
- 16 Krongauz, V. V. and Yohannan, R. M. *Polymer* 1990, **31**(6), 1130
- 17 Krongauz, V. V., Schmelzer, E. R. and Yohannan, R. M. *Polymer* 1991, **32** (9), 1654
- 18 Foster, R. 'Organic Charge-Transfer Complexes', Organic Chemistry Series, Academic Press, London, 1969
- 19 Sperling, L. H. 'Interpenetrating Networks and Related Materials', Plenum, New York, 1981
- 20 Smothers, W. K., Monroe, B. M., Weber, A. M. and Keys, D. E. 'Practical Holography IV', *SPIE OE/Lase Conf. Proc.* 1990, **1212**, 20
- 21 Krongauz, V. V. and Yohannan, R. M. *SPIE Conf. Proc.* 1990, **1213**, 174
- 22 Billingham, N. C., Calvert, P. D. and Uzuner, A. *Polymer* 1990, **31**, 258